On Line Measurement of Crystallinity of Nylon 6 Nanocomposites by Laser Raman Spectroscopy and Neural Networks

Z. Ergungor,[1] C. Batur,[2] M. Cakmak[1]

[1]*College of Polymer Engineering and Science Department of Polymer Engineering University of Akron, Akron, Ohio 44325-0301*
[2]*College of Engineering Department of Mechanical Engineering, University of Akron, Akron, Ohio 44325-3903*

Received 16 July 2003; accepted 29 September 2003

ABSTRACT: A neural network is trained to estimate the unknown crystallinity and temperature of Nylon 6 and its nanocomposites while the material is undergoing cooling at a fixed rate. The innovation of the work is that the full spectrum captured by the laser Raman spectroscope is used to train a neural network for estimation of crystallinity and temperature. The small-angle light scattering (SALS) and differential scanning calorimetry (DSC) data were used to provide the training examples for the neural network. Results indicate that the neural network can provide reliable estimates of the crystallinity and temperature provided that there is a sufficient number of training data available. Neural network methodology is also efficient in establishing the crystallization–temperature relationship as a function of cooling rate and demonstrates the heterogeneous nucleation effect of nanoclay in the nylon 6 matrix. © 2004 Wiley Periodicals, Inc. J Appl Polym Sci 92: 474–483, 2004

Key words: Raman spectroscopy; neural network; crystallization; nylon 6; nanocomposites

INTRODUCTION

The crystallinity of a polymer influences many of its characteristics, including mechanical strength, opacity, permeability, and thermal properties. In practice, crystallinity measurements are performed for research and development as well as for quality control after the materials are produced. It is advantageous to be able to measure this property as the material is being produced. This real-time determination and ultimate control of crystallinity during polymer processing provides a significant new capability to control the ultimate properties.

There is a wide range of techniques available to determine crystallinity. These include differential scanning calorimetry (DSC), density, infrared spectroscopy, small-angle light scattering (SALS), and wide-angle X-ray diffraction (WAXD), all of which have a range of requirements typically not conducive to rapid real-time crystallinity measurements. WAXD is the exception when used with synchrotron, where intensity of X-rays is large enough to acquire signal with adequate intensity to capture crystallinity information; however, this method is not very efficient at estimating the low-crystallinity levels.[1,2] Other techniques also have drawbacks. For example, SALS can be used only on thin (in the order of 5–20 μm) films. On the other hand, it is known that Raman spectral envelopes vary in intensity, position, or width when the crystallinity, temperature, stress, and orientation of a polymer are altered by the processing history.[3,4] Raman spectroscopy is an efficient method for online determination of crystallinity because it requires minor sample preparation and is fast. Raman analysis may be carried out on any sample regardless of size and location through the use of fiber optics. There have been successful off-line studies on assessing the crystallinity of polymers via Raman spectroscopy.[5–17]

Previous studies on the Raman spectra of various polymers have shown that crystallinity determination requires careful curve fitting and subsequent analysis of specific Raman vibrational modes.[5–17] In this study, we avoid concentrating on unique Raman peaks but involve the whole Raman spectrum; thus, all changes in the intensity, position, and width are used by the Neural Network methodology. Concisely, in the proposed methodology, the Raman spectrum is the input to the neural network. A set of adjustable parameters are adjusted to obtain the desired output from the neural network, in this case, the crystallinity and temperature. We term the whole experimental and estimation procedure as Raman spectroscopy with neural network (RANN). Initial studies have also been successfully conducted on other systems.[16,18]

Correspondence to: M. Cakmak (batur@uakron.edu).
Contract grant sponsor: College of Engineering at the University of Akron.

Numerous polymer processes such as fiber spinning and sheet extrusion involve cooling of material from the melt that results in crystallization that spans a certain spatial range along the process.[19–21] Heat evolution during the crystallization usually is reflected in the changes of the temperature profile along the sheet and/or fibers and this can be detected with an infrared camera. In this study, we will not only determine the crystallinity but also determine the spatial variation of temperature based solely on RANN, without the use of external methods. Our ultimate goal is to perform online crystallinity and temperature measurements via Raman spectroscopy during fiber spinning of nylon 6 and nylon 6 nanocomposites. An original study has been performed by Dupee et al. on the fiber spinning of nylon 6,6.[17] In this article, we present our preliminary studies on crystallization from the melt to avoid the effects of stress and orientation involved in fiber spinning.

EXPERIMENTAL

In this study, pure nylon 6 and nylon 6 nanocomposites with 3 and 5 wt % montmorillonite clay, purchased from RTP Co. (www.rtpcompany.com), were used. Compression-molded samples of bulk nylon 6, and nylon nanocomposites, were molten on a hot stage (at 240°C) and cooled down at specific cooling rates of 5, 7, 10, and 12°C/min. As a result, we were able to follow the influence of cooling rate on the crystallization behavior of these three materials via Raman spectroscopy. It is now well established that the presence of nanoclay in a polymer matrix affects its crystallization behavior because the additive acts as a nucleating agent.[6] This causes the crystallization to take place at higher temperatures as compared to unfilled polymer and the degree of crystallinity to become larger as well. The Raman spectra and the temperature were recorded at specific time intervals during the cooling process until the room temperature is reached. To train a neural network with respect to crystallinity and temperature, calibration data have to be constructed through an independent crystallinity measurement technique. In this study, a combination of SALS and DSC methods are used as the independent crystallinity measurement techniques. By use of SALS and DSC, the crystallinity at a given time during cooling from the melt is calculated, which in turn is used as the true crystallinity, corresponding to the Raman spectrum. A set of paired data for crystallinity, true crystallinity, and the corresponding Raman spectrum and a set of paired data for temperature, actual temperature, and the corresponding Raman spectrum are used as the neural network training data.

Calibration of crystallinity by SALS and DSC

SALS measurement device consists of a laser light source, a polarizer, a thin polymer film, and an analyzer. When crystallites form, they give rise to scattering, and depending on the relative polarization directions and the type of crystallite morphology, the angular dependency of the scattering pattern varies. The scattered light depends on the angle between polarizer (P) and analyzer (A). If P and A are parallel (V_v and H_H), the scattering is termed polarized, and if they are crossed (H_v and V_H), the scattering is depolarized, which depends on the fluctuations of optical anisotropy and orientation. In these experiments, we used the depolarized light intensity, H_v method.

The SALS analysis is based on the assumption that the polymer develops three-dimensional, spherically symmetrical clusters of crystalline and noncrystalline polymer-labeled spherulites. The analysis by Koberstein et al.[22] represents the total integrated light-scattering intensity from polymeric solids with respect to the crystallization kinetics. To discuss the crystallization kinetics from SALS, it is convenient to use the total integrated scattered intensity (invariant) defined as $Q = \int_0^\infty I(q)q^2dq$, where q is the scattering vector given from $q = (4\pi/\lambda_r)\sin(\theta)$, where λ_r is the wavelength of radiation and 2θ is the scattering angle between the incident and scattered ray. The H_v invariant (Q_{Hv}) is proportional to the mean square anisotropy within spherulites δ^2 by

$$Q_{H_v} = \frac{K}{15}\langle\delta^2\rangle \tag{1}$$

where K is a product of physical constants.

The value of δ^2 for a random assembly of spherulites in an isotropic matrix is related to the volume fraction ϕ_S of spherulites and the spherulite anisotropy $(\alpha_r - \alpha_t)_s$ by:

$$\langle\delta^2\rangle = \phi_s(\alpha_r - \alpha_t)_s^2 \tag{2}$$

where α_r and α_t are the radial and tangential polarizabilities, respectively. In other terms

$$\langle\delta^2\rangle = \phi_s[\phi_{cr,s}f_{cr,s}\delta_{cr}^0 + (1 - \phi_{cr,s})f_{am,s}\delta_{am}^0 + \delta_F]^2 \tag{3}$$

where $\phi_{cr,s}$ is the volume fraction crystallinity within a spherulite, $f_{cr,s}$ and $f_{am,s}$ are the orientation correlation functions of the crystalline and noncrystalline segments with respect to the radius of the spherulite, and δ_{cr}^0 and δ_{am}^0 are the intrinsic anisotropy of the crystalline and amorphous portions, δ_F represents the form anisotropy arising from the effect of the crystal–amorphous boundary on the internal field, which is

assumed to be negligible. Thus, a measure of the invariant could serve as a measure of the degree of the crystallinity of the sample.

When the sample is fully molten, scattering does not occur, and while the material cools down, scattering invariant increases in proportion to the formed crystallites having dimensions comparable with the wavelength of the light. This method is particularly sensitive to changes at the early stages of crystallization.

Consequently, assuming that there is a linear relation between the total light intensity (transmitted and scattered) and crystallinity of the material, the following steps constitute the calibration process:

1. A thin (20 μm) polymer piece is molten at 240°C for 10 min on a hot stage to reach a complete amorphous state, making it independent of the previous thermal history.
2. The hot stage is programmed to cool down at a particular cooling rate to 30°C. A CCD camera captures the image and the total intensity of the image is determined every 12 s.
3. The total intensity (scattered and transmitted) is assumed to be proportional to crystallinity. When the total intensity is plotted with respect to time (or temperature), it follows a sigmoidal curve, according to the generalized Avrami equation[23]

$$\phi = 1 - e^{-\int_0^t K(T(\tau))\, dr} \tag{4}$$

where ϕ is the crystallinity and the nonlinear function $K(T)$ represents the temperature dependency of the crystallization rate. When a fixed cooling rate ($dT/d\tau$) is followed as in the case of this study, the crystallinity can be written as a function of temperature as:

$$\phi = 1 - e^{-(1/(dT/d\tau))\int_0^T K(T(\tau))\, dT} \tag{5}$$

The minimum point on the sigmoidal curve represented by (5) corresponds to zero crystallinity and the maximum point corresponds to the final crystallinity.

4. The ultimate crystallinity of the film at the end of step 2 is determined by DSC in a separate experiment.
5. The sigmoidal total intensity curve is calibrated in terms of crystallinity as follows: The final (maximum) intensity value on the curve is assumed to correspond to the ultimate crystallinity value obtained in the DSC experiment of step 4. This effectively means that a linear relation is assumed between the total intensity and the material crystallinity.

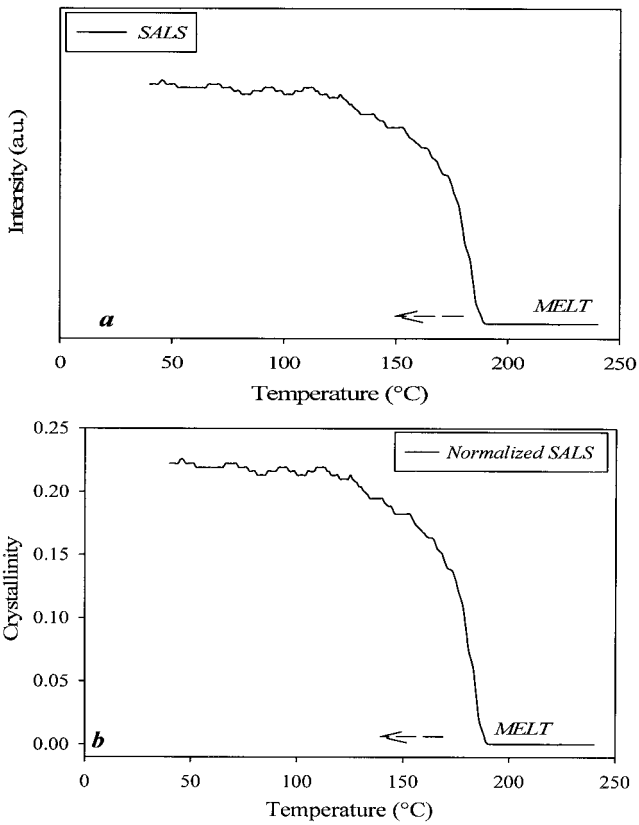

Figure 1 Changes in SALS intensity (a) and degree of crystallinity (b) during cooling from the melt for a pure nylon 6 sample cooled at 5°C/min. The degree of crystallinity is calculated by a normalization procedure based on the original SALS data in (a) and the DSC of the crystallized material (which is 22% in this case), as explained in the text.

An example of changes in light intensity in SALS with respect to cooling time and changes in crystallinity as a function of time is presented in Figure 1.

Once the true crystallinity and the true temperature at a given time during cooling are known, the neural network can be trained by using temperature–crystallinity data. When the neural network is trained, the crystallinity and the temperature can be estimated from an independent Raman spectrum by using the trained network.

Structure and training of neural network

The fundamental idea of neural networks is to adjust connection strengths (weights) between network elements (neurons) so that a particular input to the network leads to a specific target output. The structure of the network is changed by adjusting the weights so that the network learns the dynamics of the target. In this article, first the Raman spectra acquired during crystallization from the melt are analyzed. The intensity data in the regions where the most significant spectral changes occur are recorded. The Raman wave

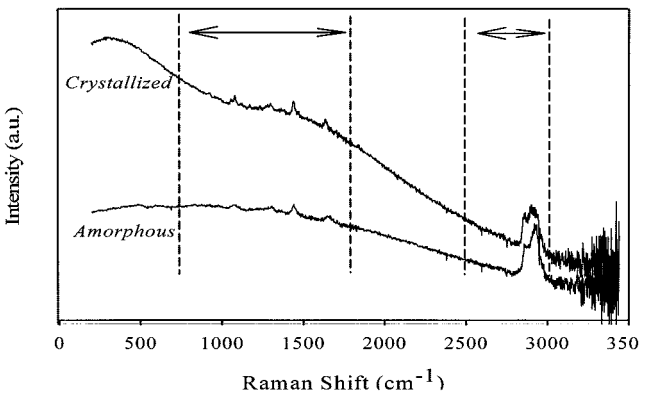

Figure 2 Raman spectra of a 3% nanocomposite sample in the melt state (amorphous) and in the crystallized state at the end of cooling at 5°C/min. The selected regions are used in training the neural network throughout the cooling process.

shifts of these regions are 700-1800 and 2500–3000 cm^{-1} for our experiments, as shown in Figure 2. The selected intensity data are first transformed into its corresponding eigenvectors and supplied to the neurons of the first layer in the neural network. The details of this initial data reduction will be given shortly. The number of training samples (spectra and the corresponding crystallinities and temperatures) depends on the cooling rate and the minimum sampling time requirements of the Raman spectrometer.

During the training phase, the spectra at a given instant are the input to the network. The outputs of the neural network are the crystallinity and temperature at the same time instant. The network is thus trained with respect to both the crystallinity and the temperature because the input Raman spectrum is dependent on the thermal history of the sample where both the crystallinity and the temperature interact. As discussed earlier, the true crystallinity is predetermined from SALS and DSC measurements, whereas the temperature is recorded according to the cooling rate. The difference between the estimated and true crystallinity as well as the discrepancy between the estimated and true temperature are used as the error signal in a back-propagation algorithm.

The training data (spectral intensities and temperatures) are normalized between 0 and 1 to avoid saturation in sigmoidal functions used by the neurons. This is performed by dividing each crystallinity value by 0.27, the maximum crystallinity achievable under the test conditions, and by dividing each temperature data by 240°C, the maximum melt temperature. The resulting crystallinities and temperatures are termed normalized percent crystallinity and normalized temperature, respectively. A general representation of the described neural network is given in Figure 3.

Our optimized neural network is created through a two-layer feed-forward back-propagation network, as shown in Figure 3. We assume that each column of the data matrix D below represents the intensities of one observed Raman spectrum at the selected wave shifts,

$$D = \begin{bmatrix} d_{1,1} & d_{1,2} \ldots d_{1,n} \\ d_{2,1} & d_{2,2} \ldots d_{2,n} \\ \ldots & \ldots \\ d_{m,1} & d_{m,2} \ldots d_{m,n} \end{bmatrix}; \quad D \in R^{mxn} \tag{6}$$

Therefore, each spectrum is represented by (m) number of spectral intensities and a total of (n) spectrum exist, typically $m \gg n$. The dispersion matrix Z that represents the variation in the data and is computed as

$$Z = D^T D; \quad Z \in R^{nxn} \tag{7}$$

Significant data compression can be achieved by expressing the data matrix D in terms of the eigenvectors of the dispersion matrix Z. To this end, we first use the singular value decomposition and express the dispersion matrix in terms of its eigenvalues and eigenvectors, for instance,

$$Z = L\lambda L^T \tag{8}$$

where L contains the eigenvectors (l_i) and λ has the eigenvalues (λ_i) of Z as

$$L = \begin{bmatrix} l_{11} & l_{21} & l_{k1} \cdot l_{n1} \\ l_{12} & l_{22} & l_{k2} \cdot l_{n2} \\ l_{1n} & l_{2n} & l_{kn} \cdot l_{nn} \end{bmatrix}; \quad \lambda = \begin{bmatrix} \lambda_1 & 0 & 0 & 0 \\ 0 & \lambda_2 & 0 & 0 \\ 0 & 0 & \cdot & 0 \\ 0 & 0 & 0 & \lambda_n \end{bmatrix} \tag{9}$$

Because the eigenvectors are orthonormal (i.e., $L^T L = LL^T = I$), we can write the data matrix as

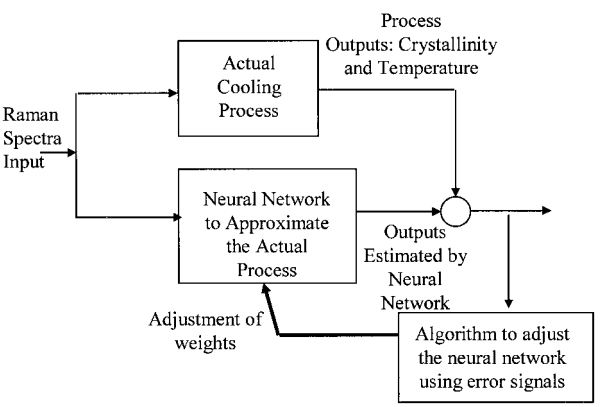

Figure 3 General structure of a neural network. The neural network receives the intensities from each Raman spectrum during cooling of a material from the melt and is trained to estimate the process outputs, which are the crystallinity and the temperature of the material in this study.

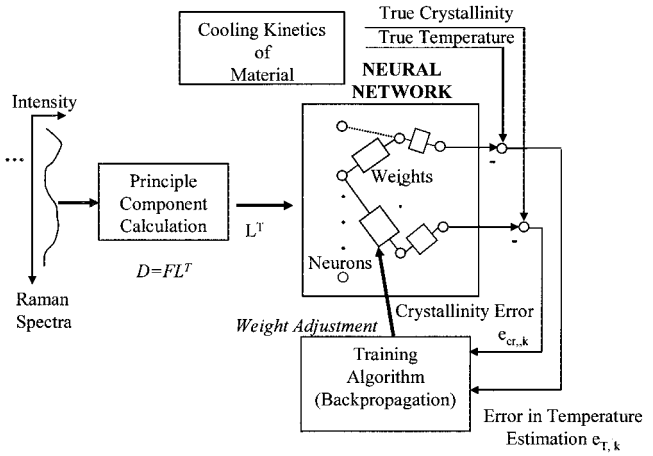

Figure 4 Structure of the neural network that uses the principal components as inputs. The input neurons of the network receives the data condensed in terms of the eigenvalues matrix L^T rather than the original Raman spectra data matrix D.

$$D = DLL^T \equiv FL^T \tag{10}$$

where $F \equiv DL \in R^{mxn}$ is the factor matrix of the Principal Component Analysis technique. The kth spectrum of the data matrix can now be written as a linear combination of the columns of the factor matrix as

$$\text{spectrum}(k) = \begin{bmatrix} d_{1,k} \\ d_{2,k} \\ \cdot \\ d_{m,k} \end{bmatrix} = \begin{bmatrix} f_{1,1} \\ f_{1,2} \\ \cdot \\ f_{1,m} \end{bmatrix} \cdot l_{k,1} + \ldots + \begin{bmatrix} f_{n,1} \\ f_{n,2} \\ \cdot \\ f_{n,m} \end{bmatrix} \cdot l_{k,n} \tag{11}$$

The coefficients ($l_{k,i}$; $i = 1, 2, \ldots, n$) in this linear expression are the elements of the eigenvectors of the dispersion matrix, as shown in eq. (6). Incidentally, these coefficients are referred to as the factor loadings in the Principal Component Analysis (PCA). One can interpret each column of the F matrix as an abstract spectrum and the eigenvectors essentially determine the contribution of each abstract spectrum into the observed spectrum. Because the eigenvectors contain condensed information about the spectrum, it is decided to use the eigenvectors (i.e., the columns of L^T matrix rather than the original data matrix D as input to the neural network). This choice significantly cuts down the number of neurons of the neural network. Therefore, we are effectively using the PCA to reduce the complexity of the required neural network. The final structure of the neural network is shown in Figure 4. The network receives the selected portion of the Raman spectrum, D matrix, and condenses the data in terms of the eigenvalues matrix L^T on its input neurons.

The transfer function of a typical neuron is chosen as a sigmoid function. For example, for a neuron on the first hidden layer, the neuron output is given as

$$y_j = f\left(\sum_{i=1}^{i=m} w_{ij}x_i + b_i\right); \quad j = 1, 2, \ldots, J; \quad \text{and} \quad f(\cdot) = \frac{1}{1 + e^{-(\cdot)}} \tag{12}$$

The performance index PI of training is defined as the sum of squares of the estimation error for a total of N training samples, for instance,

$$PI = \frac{1}{2}\left(\sum_{k=1}^{N} e_{cr,k}^2 + e_{T,k}^2\right) \tag{13}$$

where $e_{cr,k}$ is the difference between the true (from SALS/DSC measurement) and the estimated crystallinity (from neural network) and $e_{T,k}$ is the difference between the true (from cooling rate) and the estimated temperature (from neural network). In our training, we set the PI as 0.00001. The training stops when this goal is achieved or a maximum iteration of 1000 is reached.

The subroutine TRAINLM of the Matlab neural network toolbox is used to implement the training algorithm. Further details of the algorithm can be found in refs. [24] and [25].

RESULTS AND DISCUSSION

The discussion of the results will be summarized in two sections:

1. Training and testing is based on all available cooling data. The data, corresponding to all cooling rates, are divided into two sections and one section is used for training the neural network and the other section is used for evaluating the performance of the trained neural network.
2. Training is based on part of the cooling rate data and testing is based on the rest of the cooling data. For example, the 5, 7, and 10°C/min cooling rate data are used to train the network, whereas the 12°C/min cooling rate data are used to test the performance of the neural network.

Although the training stops when a performance index PI of 0.00001 (or a maximum iteration of 1000) is reached, the crystallinities and temperatures esti-

mated by the network are not necessarily guaranteed to be at their optimum values. Training with different initial conditions can give entirely different simulation results with an even lower performance index. This is due to the fact that the neural network training is essentially a minimization of a nonlinear function; therefore, the final structure of the neural network depends on the initial structure of the network as well as the topology of the function minimized. We calculated the average errors and standard deviation of crystallinity and temperature estimates in all the data sets obtained. The results presented will be based on the data with minimum average error and standard deviation. For example, the average error and standard deviation for crystallinity data are calculated according to

$$\text{error}_i = \text{crystallinity}_{\text{estimated},i} - \text{crystallinity}_{\text{actual},i} \tag{14}$$

$$\text{Average Error} = \frac{1}{N}\sum_{i=1}^{N} \text{error}_i \tag{15}$$

$$\text{Standard Deviation} = \sqrt{\frac{1}{N}\sum_{i=1}^{N} (\text{error}_i - \text{Average Error})^2} \tag{16}$$

where the subscript i refers to each crystallinity data and N is the total number of crystallinity values in the data set.

Results on training and testing based on all cooling rate data

Figure 5 illustrates an example on how the network is trained in terms of the normalized crystallinity [Fig. 5(a)] and normalized temperature [Fig. 5(b)] training data for the 3% nanocomposite samples. The training data contains half of all the calibration data (i.e., in each spectrum the data is divided into two halves); the odd numbered data are used for training and the even numbered data are used for testing, as shown below:

$$\text{Spectrum Intensities} = [d_{1,i}, d_{2,i}, d_{3,i}, d_{4,i}, \ldots, d_{(m-1),i}, d_{m,i}]^T$$

$$\text{Training data} = [d_{1,i}, d_{3,i}, \ldots, d_{(m-1),i}, d_{m,i}]^T$$

$$\text{Testing data} = [d_{2,i}, d_{4,i}, \ldots, d_{m,i}]^T$$

The data considered correspond to 5, 7, 10, and 12°C/min cooling rates. All the estimated and the actual crystallinities as well as temperatures are represented as a function of the selected training data. Figure 5(a, b) prove how one can be successful in training a network to correctly estimate crystallinity and temperature in the training data. The number of sampled data decreases for the increased cooling rates because capturing a fluorescent-free spectrum requires at least 30 s, therefore limiting the number of samples for the increased cooling rates. According to Figure 5(a), for each cooling rate the crystallinity increases smoothly and then levels off, thus following a sigmoidal curve as expected. According to Figure 5(b), the temperature decreases linearly and the slope of the curve changes based on the cooling rate, again as expected.

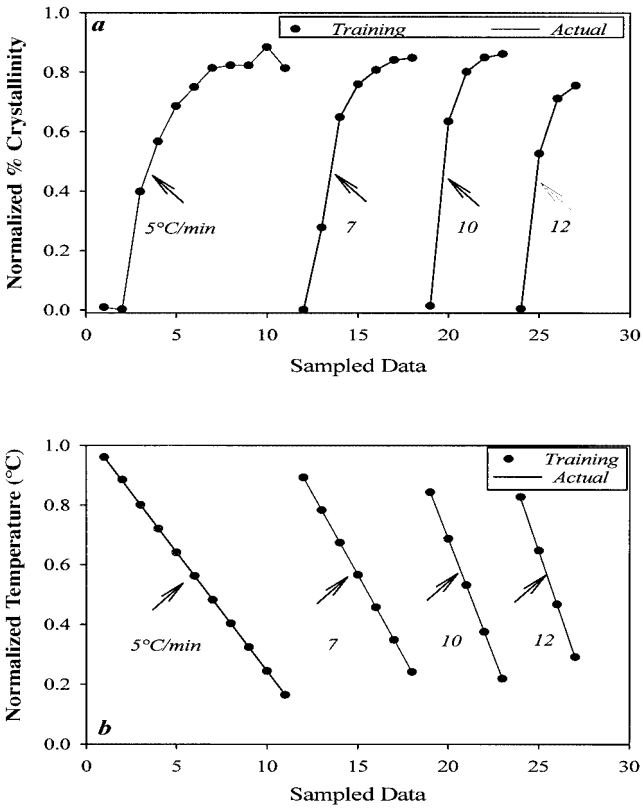

Figure 5 Trained neural network output and actual data for normalized % crystallinities (a) and normalized temperatures (b) for the 3% nanocomposite samples cooled at 5, 7, 10, and 12°C/min. The training data contain half of all the calibration data, where the odd numbered data of the collected spectra are used for this figure.

Next, the trained neural network is used to estimate the crystallinity and temperature for the testing data, which contains the other half of the whole calibration data (even-numbered data in each data set) for 5, 7, 10, and 12°C/min cooling rates. The results are given in Figure 6. It is important to note here that the testing data was not used by the neural network during training. Figure 6(a) represents the estimated and actual normalized crystallinities for each chosen testing data, whereas Figure 6(b) reveals the corresponding nor-

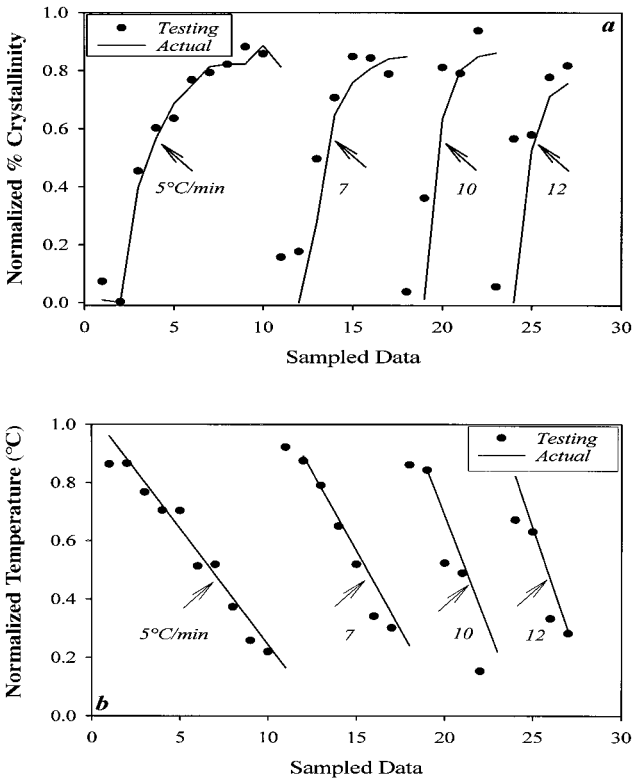

Figure 6 Simulated (based on the trained network of Fig. 5) and actual normalized % crystallinities and temperatures for the 3% nanocomposite samples cooled at 5, 7, 10, and 12°C/min. The testing data contain the other half of all the calibration data, where the even-numbered data of the collected spectra are used for this figure.

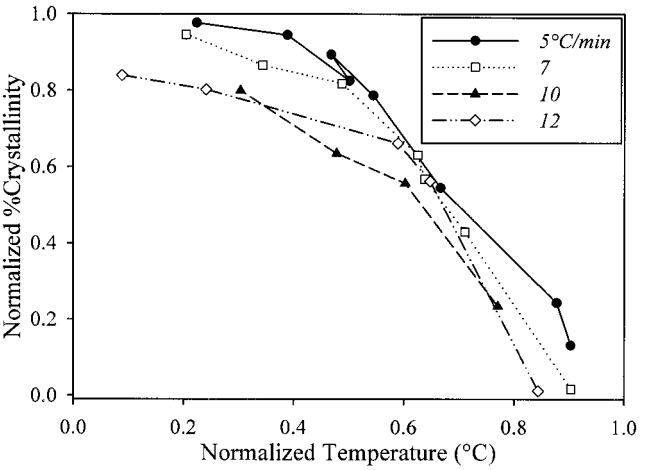

Figure 7 The normalized % crystallinity for the 5% nanocomposites cooled at 5, 7, 10, and 12°C/min as a function of normalized temperature. This figure displays the effect of cooling rate on the crystallization kinetics.

malized temperatures. We can easily observe how the neural network methodology generates reliable results in estimating crystallinity and temperature based on a given Raman spectrum once an accurate training has been established. The dependence of crystallinity and temperature on cooling rate is very well captured by the neural network. The average error and standard deviation for crystallinity and temperature corresponding to the training and testing data are given in Table I. The errors and standard deviations are truly minor in the training data and satisfactorily small for the testing data.

An important purpose to fulfill in this study is to ensure that we are capable of following the effect of cooling rate on crystallization. As the rate of cooling increases from 5 to 12°C/min, the crystallization is expected to be induced at lower temperatures as a result of supercooling. Additionally, when the samples are cooled at slower cooling rates, they attain higher crystallinity levels because they spend more time at higher temperatures.

Figure 7 displays the normalized percent of crystallinity for the 5% nanocomposite as a function of normalized temperature at various cooling rates. It is obvious that the RANN demonstrates the fact that while cooling from the melt, crystallinity development follows a sigmoidal curve with respect to temperature; it increases smoothly over a certain temperature range and then levels off. At lower cooling rates, the crystallization starts at higher temperatures and crystallinity content reaches higher values than faster cooling rates. Evidently, RANN is an efficient method to estimate crystallinity and temperature and to confirm their relationship in a cooling process.

The effect of nanoclay addition to the nylon 6 matrix is observed in Figure 8, where the normalized crystallinity–temperature curve is presented for the samples cooled down at 12°C/min. The nanocomposites begin to crystallize at temperatures higher than pure nylon 6

TABLE I
The Average Error and Standard Deviation, Calculated According to the Eqs. (14)–(16), for Percent Crystallinity and Temperature on the Training and Testing Data for the 3% Nanocomposite Samples

	Crystallinity		Temperature	
	Average error	Standard deviation	Average error	Standard deviation
Training data	-3.89×10^{-4}	9.80×10^{-4}	1.63×10^{-4}	0.0013
Testing data	−0.0065	0.0781	−0.0101	0.0668

The cooling rates from the melt state are 5, 7, 10, and 12°C/min.

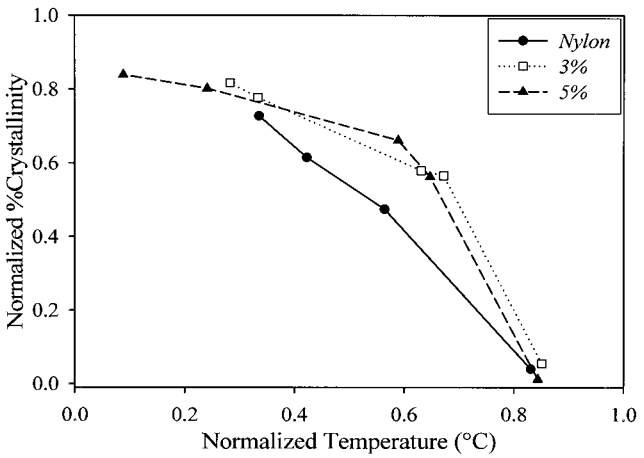

Figure 8 The normalized % crystallinity for the pure nylon 6, 3, and 5% nanocomposites cooled at 12°C/min as a function of normalized temperature. This figure illustrates the effect of the nanoclay in a nylon 6 matrix when crystallization develops from the melt.

and they also display larger crystallinity levels throughout the whole cooling process. Thus, the RANN method is successful in confirming the general nanocomposite behavior.

In this section, we observed that when a sufficient number of data are used to train a neural network, we are able to successfully estimate the crystallinities and temperatures for a range of cooling rates. In the next section, we will investigate if the neural network would be successful at the extreme ends of cooling rates at which the network was not provided with the training data, for example, if the network would be able to estimate crystallinities for 12°C/min cooling rate if the training data did not have such a high cooling rate. The next section describes the behavior of network under this condition.

Results on training and testing based on part of the cooling rate data

Figure 9 describes the performance where that the network is trained on only 5, 7, and 10°C/min cooling rates and the trained network is asked to estimate the actual crystallinity and temperature data for the 3% nanocomposite samples cooled down at 12°C/min. It is clear that the network successfully captures the increase in sample crystallinity following a sigmoidal curve [Fig. 9(a)] and the linear decrease in temperature [Fig. 9(b)]. The average errors and standard deviations given in the figure show that the estimations are quite reliable. The same observations are also valid for the simulation on the 3% nanocomposite samples cooled at 5°C/min (Fig. 10), where the data included in the training data corresponded to the samples cooled only at 7, 10, and 12°C/min. The average errors are slightly better, because a larger number of Raman spectra are collected at slower cooling rates. Consequently, we have shown that the RANN is capable of capturing the fundamental relation between the temperature history and the crystallinity.

To further analyze how the neural network captures the dynamics, the 7°C/min data for pure nylon samples have been omitted deliberately for the next set of experiments. First, we tried to estimate the crystallinity and temperature for the 12°C/min cooling rate data with a network trained with 5 and 10°C/min rate of cooling. Figure 11(a) presents the normalized percent of crystallinity data and their comparison to the actual data and Figure 11(b) summarizes the results on the normalized temperature. It is evident that the outcome is still satisfactory. However, when we try to approximate the crystallinity and temperature of the samples cooled down at 5°C/min based on the training with 10 and 12°C/min data, the RANN method is not successful. The crystallinity does not increase fol-

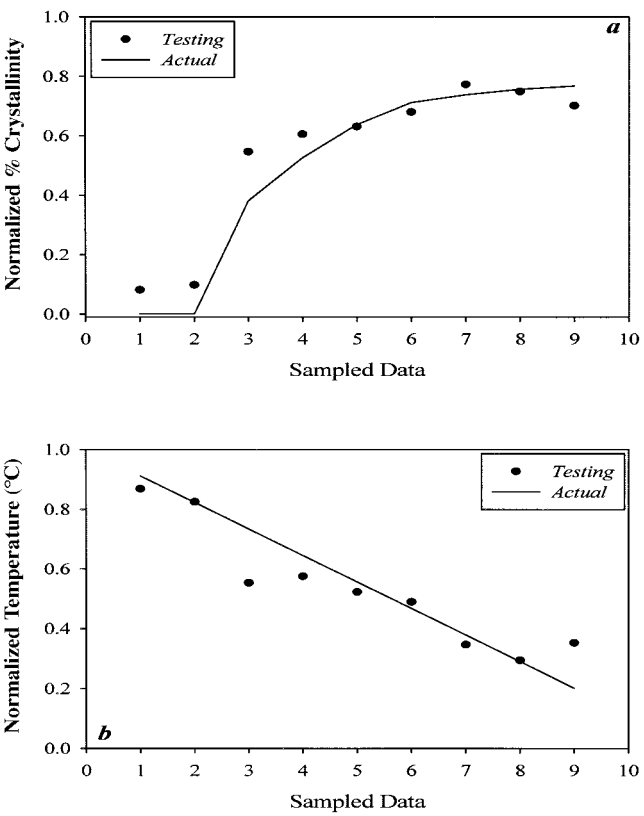

Figure 9 The normalized % crystallinity and normalized temperature for the 3% nanocomposite samples cooled at 12°C/min. The training is based on the 5, 7, and 10°C/min cooling rates data. (a) Testing of the normalized % crystallinity by neural network simulation. The error and standard deviation relative to the actual crystallinity data are −0.0383 and 0.0691, respectively. (b) Testing of the normalized temperature by neural network simulation. The error and standard deviation relative to the actual temperature data are 0.0201 and 0.0825, respectively.

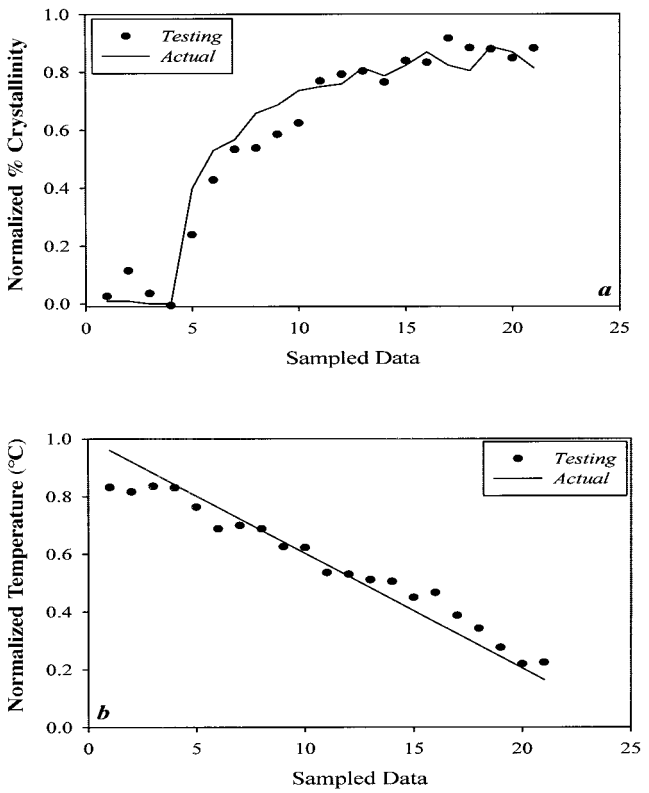

Figure 10 The normalized % crystallinity and normalized temperature for the 3% nanocomposite samples cooled at 5°C/min. The training is based on the 7, 10, and 12°C/min cooling rates data. (a) Testing of the normalized % crystallinity by neural network simulation. The error and standard deviation relative to the actual crystallinity data are −0.0125 and 0.0713, respectively. (b) Testing of the normalized temperature by neural network simulation. The error and standard deviation relative to the actual temperature data are −0.0014 and 0.0657, respectively.

lowing a sigmoidal curve [Fig. 12(a)] and the temperature does not decrease linearly [Fig. 12(b)]. The standard deviations especially are quite large. It is most probably not very reliable to try to reproduce a large number of data points (20 points for the 5°C/min cooling rate data) based on training with a limited number of data points. Additionally, we did not include the data close (7°C/min) to the cooling rate data in question (5°C/min) and this obviously affects the outcome seriously.

CONCLUSION

This article is an extension of the previous study[18] on the application of RANN to measure the crystallinity of a polymeric material online and nonintrusively while the sample is cooled from the melt at a fixed cooling rate. The advantage of the Neural Network is that it makes use of the whole Raman spectrum in calculating the crystallinity rather than concentrating on the unique Raman peaks as is common in the literature. We contribute to the technique introduced by Batur et al.[18] on two additional aspects:

(1) The neural network is trained with respect to crystallinity as well as temperature by using selected regions of Raman spectra corresponding to specific cooling rates input to the network. The trained network is then used to estimate crystallinity and temperature simultaneously based on any other given Raman spectrum. This new step would eliminate the use of an external method such as infrared camera to determine the cooling history of a material in an actual process such as fiber spinning.

(2) RANN methodology is applied to nylon 6 and nylon 6 nanocomposite samples. The aim was to investigate the effect of nanoclay addition on the crystallization of the polymer matrix.

Our technique performs very satisfactorily on training a neural network to estimate crystallinity and temperature of a sample based on its Raman spectrum recorded at a given time during cooling from the

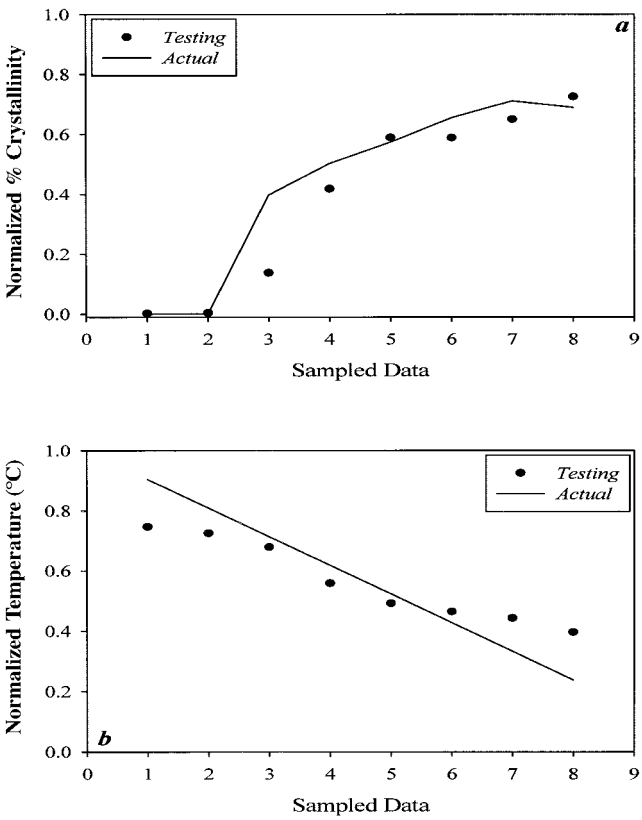

Figure 11 The normalized % crystallinity and normalized temperature for the pure nylon 6 samples cooled at 12°C/min. The training includes only 5 and 10°C/min cooling rate data. (a) Comparison of the normalized % crystallinity simulated by neural network to the actual crystallinity data. The error and standard deviation are 0.0554 and 0.0872, respectively. (b) Comparison of the normalized temperature simulated by neural network to the actual temperature data. The error and standard deviation are 0.0079 and 0.0974, respectively.

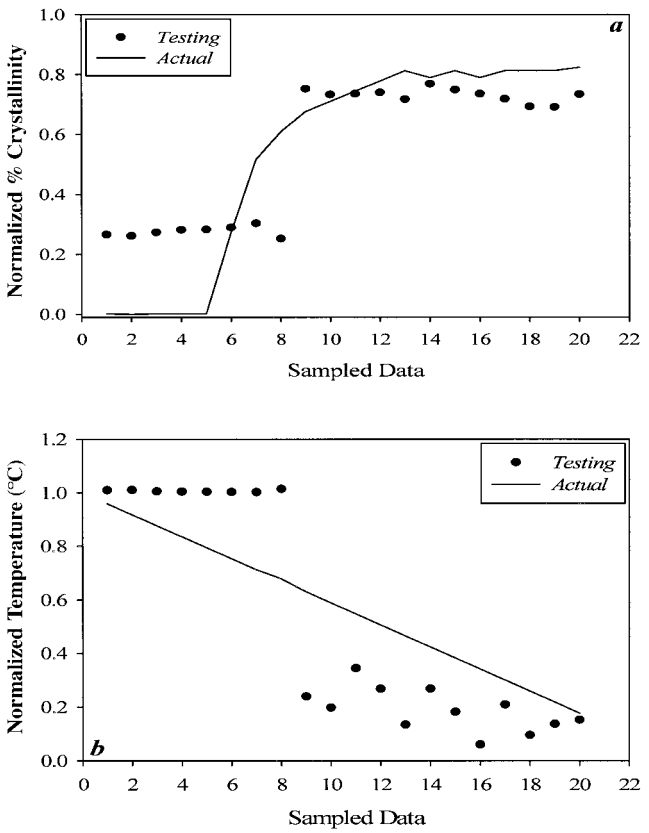

Figure 12 The normalized % crystallinity and normalized temperature for the pure nylon 6 samples cooled at 5°C/min. The training includes only 10 and 12°C/min cooling rate data. (a) Comparison of the normalized % crystallinity simulated by neural network to the actual crystallinity data. The error and standard deviation are 0.0102 and 0.1747, respectively. (b) Comparison of the normalized temperature simulated by neural network to the actual temperature data. The error and standard deviation are 0.0509 and 0.2249, respectively.

amorphous state. The trained network is then successfully used to determine these parameters on various samples cooled down at the same or different cooling rates. This technique lets us follow the dependence of crystallinity and temperature on cooling and cooling rate: As the temperature decreases, the estimated crystallinity increases smoothly over a certain temperature (time) range and levels off. Also, as expected, the temperature decreases linearly with a changing slope according to the cooling rate. We are also able to confirm that the crystallization is induced at a lower temperature as the cooling rate increases and that those samples attain a lower degree of crystallinity.

RANN has also proved to be a useful method in confirming the general nanocomposite crystallization behavior: The nanocomposites begin to crystallize at temperatures higher than the bulk polymer and display larger crystallinity levels during the entire cooling process.

An important observation is that one needs a sufficient number of data points to train the neural network to effectively estimate the crystallinities and temperatures. One also needs to cover a large range of cooling rates to simulate the process parameters at the extreme conditions to capture the fundamental relation between crystallinity and the temperature history. In an actual process such as fiber spinning, the cooling rate and initial conditions may not be identified *a priori*. Consequently, one needs to include a wider range of supplementary processing conditions; otherwise, the network may capture only a partial information about the process dynamics.

The first author thanks the College of Engineering at the University of Akron for financial support.

References

1. Alexander, L. E. X-ray Diffraction Methods in Polymer Science; Wiley-Interscience: New York, 1969.
2. Kellar, E. J. C.; Evans, A. M.; Knowles, J.; Galiotis, C.; Andrews, E. H. Macromolecules 1997, 30, 2400.
3. Delhaye, M.; Dhamelincourt, P. Microbeam Anal 1990, 25, 220.
4. Bulkein, B. J. in Polymer Applications, Analytical Raman Spectroscopy; Grasselli, J. G.; Bulkin, B. J., Eds.; Wiley: New York, 1991; Vol. 114, p. 317.
5. Melveger, A. J. J Polym Sci, Part A-2 1972, 10, 317.
6. Strobl, G. R.; Hagedorn, W. J Polym Sci, Polym Phys Ed 1978, 16, 1181.
7. Bulkin, B. J.; Lewinn, M.; DeBlase, F. J. Macromolecules 1985, 18, 2587.
8. Adar, F.; Noether, H. Microbeam Anal 1985, 20, 41.
9. Foldes, E.; Keresztury, G.; Iring, M.; Tudos, F. Angew Makromol Chemie 1991, 187, 87.
10. Everall, N.; Tayler, P.; Chalmers, J. M.; MacKerron, D.; Ferwerda, R.; Van der Maas, J. H. Polymer 1994, 35, 3184.
11. Ellis, G.; Roman, F.; Marco, C.; Gomez, M. A.; Fatou, J. G. Spectrochim Acta, Part A 1995, 51, 2139.
12. Williams, K. P. J.; Everall, N. J. J Raman Spectrosc 1995, 26, 427.
13. Lehnert, R. J.; Hendra, P. J.; Everall, N. Polym Commun 1995, 36, 2473.
14. Rull, F.; Rodriguez, J.; Alia, J. M.; Arroyo, F.; Edwards, H. Macromol Symp 1995, 94, 189.
15. Kellar, E. J. C.; Galiotis, C.; Andrews, E. H. Macromolecules 1996, 29, 3515.
16. Cakmak, M.; Serhatkulu, T.; Graves, M.; Galay, J. ANTEC Proc 1997, 2, 1794.
17. Dupee, J. D.; Galiotis, C.; Davidson, D. L. U.S. Pat. 5,999,255, 1999.
18. Batur, C.; Vhora, M. H.; Cakmak, M.; Serhatkulu, T. ISA Trans 1999, 38, 139.
19. Bansal, V.; Sjambaugh, L. Polym Eng Sci 1996, 36, 2785.
20. Leephakpreeda, T.; Batur, C. Int Polym Proc 1997, 12, 373.
21. Liu, L.; Qi, Z.; Zhu, X. J Appl Polym Sci 1999, 71, 1133.
22. Koberstein, J.; Russell, T. P.; Stein, R. S. J Polym Sci, Polym Phys Ed 1979, 17, 1719.
23. Avrami, M. J Chem Phys 1939, 7, 1103; Avrami, M. J Chem Phys 1940, 8, 212; Avrami, M. J Chem Phys 1941, 9, 177.
24. Kasparian, V.; Batur, C. ISA Trans 1998, 37 (1), 21–39.
25. Neural Network Toolbox, Version 3; The MathWorks, Inc., 1998.